



Elimination Study of Anionic Dye by Co-products of the Phosphate Industry: Kinetics and Thermodynamic

Mohammed Mehnaoui ^a, Mustapha Hidouri ^{b*} and Khaled Boughzalaa ^c

^a Applied Chemistry to Natural Resources Substances and to the Environment Laboratory, Carthage University, Faculty of Sciences of Bizerte, 7021 Zarzouna, Bizerte, Tunisia.

^b High Institute of Applied Sciences and Technology, 6072 Zrig, Gabes University, Tunisia.

^c RU Analysis and Applied Process for Environment, High Institute for Applied Sciences and Technology, 5121 Mahdia, Tunisia.

Authors' contributions

This work was carried out in collaboration among all authors. All authors read and approved the final manuscript.

Article Information

DOI: 10.9734/IRJPAC/2021/v22i1230449

Open Peer Review History:

This journal follows the Advanced Open Peer Review policy. Identity of the Reviewers, Editor(s) and additional Reviewers, peer review comments, different versions of the manuscript, comments of the editors, etc are available here: <https://www.sdiarticle5.com/review-history/85174>

Original Research Article

Received 20 October 2021
Accepted 28 December 2021
Published 30 December 2021

ABSTRACT

Water is essential for all living things however its pain has become serious. Many industrial activities cause pollution by the release of polluting byproducts. Wastewater treatment is hence necessary. In this context, the wastewater of the textile industry containing Red Acid 52 was treated by the solid waste of the washed natural phosphate byproduct. Natural phosphate was also studied. The solid materials were first characterized by chemical analysis, Fourier Transform Infrared spectroscopy (FTIR), and X-ray diffraction (XRD). The phosphate materials were after that, tested in the adsorption of the Red Acid 52. The experimental data indicated that the phosphate waste rock allowed the removal of Red Acid 52. Its maximum retention capacity attained 18.4 mg.g⁻¹. Calcinations of materials inhibit the removal capacity found reduced by 60 to 70%. The adsorption kinetics of the Red Acid 52 on the material is well described by the pseudo-second-order model while the adsorption isotherms are identified by the Langmuir model. Hereafter, the thermodynamic study revealed that the adsorption process is spontaneous and exothermic. The obtained results indicated that the adsorbent has the best adsorption capacity of 18.4 mg.g⁻¹. The removal quantity decreases when the adsorbent is calcined. The kinetics model most appropriate is the pseudo-

*Corresponding author: E-mail: mustapha.hidouri@laposte.net;

second-order model. As for the adsorption isotherms, they are well described by the Langmuir model. The temperature effect indicates a decrease in the adsorbed amount with the increase of temperature. Furthermore, the adsorption is spontaneous and exothermic and the reaction is physical in nature for both materials.

Keywords: Wastewater; phosphate co-product; adsorption; red Acid 52.

1. INTRODUCTION

The activities of textile dyers are responsible for the significant pollution of residual water. These water discharges, which are very loaded with synthetic dyes, usually exhibit a disturbing, intense coloring and high toxicity, especially when they are discharged directly into nature or into sewerage pipes. With the emergence of new standards and increasingly stringent environmental legislation, water discharges will imperatively require treatment to reduce or even eliminate their coloring and their pollutant load before being discharged into nature.

The literature reports several techniques for the treatment and de-pollution of waste textile effluents. To quote membrane filtration techniques [1], coagulation/flocculation [2], electrocoagulation [3], advanced oxidation techniques [4-6] and aerobic and anaerobic biological processes [7-9]. For economic and technical reasons, most of these techniques have not given satisfactory results. Moreover, adsorption is one of the most attractive remediation techniques in recent decades [2]. Although activated carbon remains the most effective adsorbent, its price, still considered high, prompts researchers to find other alternative and inexpensive materials. Most of these materials are natural [10-16] or from waste agriculture and other industries such as, for example, the food industry [17-21].

This last approach consists in recovering waste from various industries and applying it in the decontamination of wastewater discharges. This become a very emerging ecological concept and very widespread in the world of scientific research since it is part of the sustainable development framework.

Solid waste from the phosphate industry found in abundance in Tunisia, is currently a national environmental problem. This is why it seemed interesting to use it in the decontamination of wastewater discharges. Indeed, the literature reveals the existence of few studies relating to the adsorption of certain textile water discharges

by phosphogypsum [22] or the adsorption of basic dyes and reactive dyes by natural phosphate [23, 24].

In this work, we are interested in synthetic acid dyes, widely used in the dyeing of wool, silk, polyamide, and even leathers and furs [25, 26]. Among these dyes, we have chosen an azo dye, Red Acid 52.

2. MATERIALS AND METHODS

2.1 Materials

Phosphate waste rock is a byproduct of a phosphate company's washing plant. Prior to use, the samples have been considerably washed with distilled water and then dried in an oven at 105°C.

The phosphate waste rock was exposed to thermal activation under nitrogen (150 mL/h) at the temperature of 1000°C at 5°C/min for 2 h.

In the following sections, the phosphate waste rock and the phosphate waste rock calcined will be assigned DS and DSC. Both compounds were intended for the removal tests of the Acid Red 52 dye. Red Acid 52 with a chemical structure developed in Fig. 1. Its molar mass is 580.65 g.mol⁻¹.

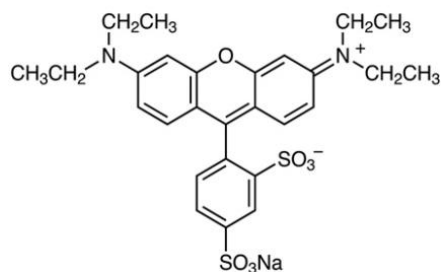


Fig. 1. Chemical structure of Acid Red 52 dye

Its absorption spectrum is shown in Fig. 2. According to this figure, its maximum absorbance A_{\max} occurs for a wavelength λ_{\max} equal to 568 nm.

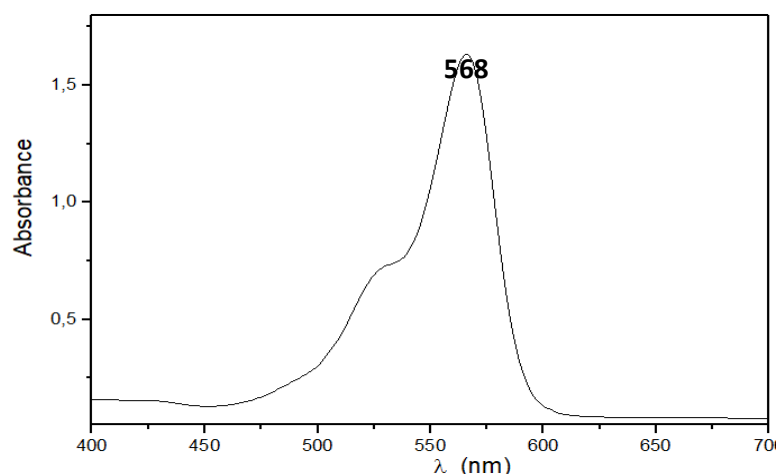


Fig. 2. Visible spectrum of the Acid Red 52 dye studied

2.2 Removal Experiments

The absorption experiments were carried out in batches with different amounts of dyes and adsorbents. In addition, to the effect of the absorbent mass, we investigated the pH effect, dye concentration, contact time, and temperature. Apart from the experiments studying the temperature all the others were carried out at room temperature. After stirring at a given speed a fixed period of time, samples were separated from the absorbent by centrifugation. After that, the samples were analyzed using UV-visible spectrophotometer type UV-2401PC at a wavelength of 568 nm. The residual dye concentration in each suspension was determined using a previously established calibration curve. The amount of adsorbed dye on the surface of the powders at time t is given by the following relationship and the percentage of discoloration by:

$$R(\%) = 100 * \left(\frac{C_0 - C_t}{C_0} \right) \quad (1)$$

$$q_t = (C_0 - C_t) \frac{V}{m} \quad (2)$$

Where C_0 and C_t are respectively the initial and residual concentrations of the dye at time t (mg.L^{-1}), V is the volume of the solution (L) and m is the mass of the adsorbent used (g).

The pH measurements were carried out using a BPH 213 type pH meter.

2.3 Characterization

The Chemical analyses of the adsorbents were carried out using an atomic absorption

spectrometer type Perkin Elmer 3110. The DRX diffractograms were recorded using a PAnalytical X'Pert Pro type diffractometer, in the 2θ range $10-60^\circ$ with a step of 0.02° and an equal counting time of 1s, using the K_α radiation of copper ($\lambda = 1.5406 \text{ \AA}$). The infrared absorption spectra were recorded using a Perki Elmer 1283 Fourier transform spectrometer using the potassium bromide (KBr) method. Gravimetric (GTA) and differential thermal analysis (DTA) were performed using a Setaram instrumentation SETSYS evolution system with a heating rate of $10^\circ\text{C}/\text{min}$ up to 1000°C under air atmosphere. The surface morphology of the samples was examined by scanning electronic microscopy (SEM, FEI Quanta 200). The specific surface area (SSA) values were estimated from nitrogen adsorption isotherms using the BET (Brunauer–Emmett–Teller) equation. The isotherms were obtained using a Micromeritics ASAP 2020 system. The samples were outgassed at 120°C for 8 h before the measurement. The concentration of AR-88 at equilibrium was determined during the removal runs using a UV-visible spectrophotometer (Perkin Elmer model LAMBDA20) at a maximum wavelength of 568 nm.

3. RESULTS AND DISCUSSION

3.1 Characterization of Adsorbents

The results of the chemical analysis, given in Table 1 showed that the concentration of CaO is equal to 26% in the DS sample. This sample has a P_2O_5 content of 14%. A small percentage of MgO, close to 0.87%, was detected. The Ca/P atomic ratio is approximately 1.91 for DS. The Cd

content was close to 45 ppm. The heat treatment did not radically change the chemical composition and a slight variation in P₂O₅ was observed as for other phosphate rocks [27].

The crystallographic identification of the DRX diagrams given in Fig. 3 reveals that the powder contained mainly as the major phase of carbonated fluorapatite (Ca_{9.55}(PO₄)_{4.96}F_{1.96}(CO₃)_{1.28}), with traces of heulandite ((C₂H₅)NH₃)_{7.85}(Al_{8.7}Si_{27.3})O₇₂(H₂O)_{6.92} and quartz (SiO₂). After calcination, at 1000 °C, no variation of the major phase was observed. Also, it is noted that calcination improves the crystallinity of the sample [27].

The FTIR spectra of the solid waste are shown in Fig. 4. The identification of bands was made with reference to similar studies [28-30]. The characteristic bands of the phosphate groups

PO₄ appearing at around 1042 cm⁻¹ were attributed to the symmetrical valence vibration mode, u₁. The bands recorded around 1090 cm⁻¹ were related to the antisymmetric valence vibration mode, u₃. Those between 520 and 570 cm⁻¹ correspond to the antisymmetric mode of deformation u₄, while those located between 400 and 470 cm⁻¹ are associated with the symmetrical mode of deformation u₂. The bands located around 1453-1406 and 863 cm⁻¹ are associated with the CO₃²⁻ group, indicating the presence of these ions in the structure of the materials [31-33]. The two bands around 3450 cm⁻¹ and 1640 cm⁻¹ are due to adsorbed molecular water on the surface of the particles [34-35]. FTIR spectra of the calcined material at 1000°C indicated that some changes occurred; the intense peak of the phosphorus group around 1036 cm⁻¹ was shifted to 1081 cm⁻¹. Moreover, the bands of the carbonate species and impurities have disappeared.

Table 1. Chemical composition of adsorbents

↓Adsorbants	%P ₂ O ₅	%CaO	%MgO	Cd (ppm)	CaO/P ₂ O ₅
DS	14	26,72	2,15	51	1,908

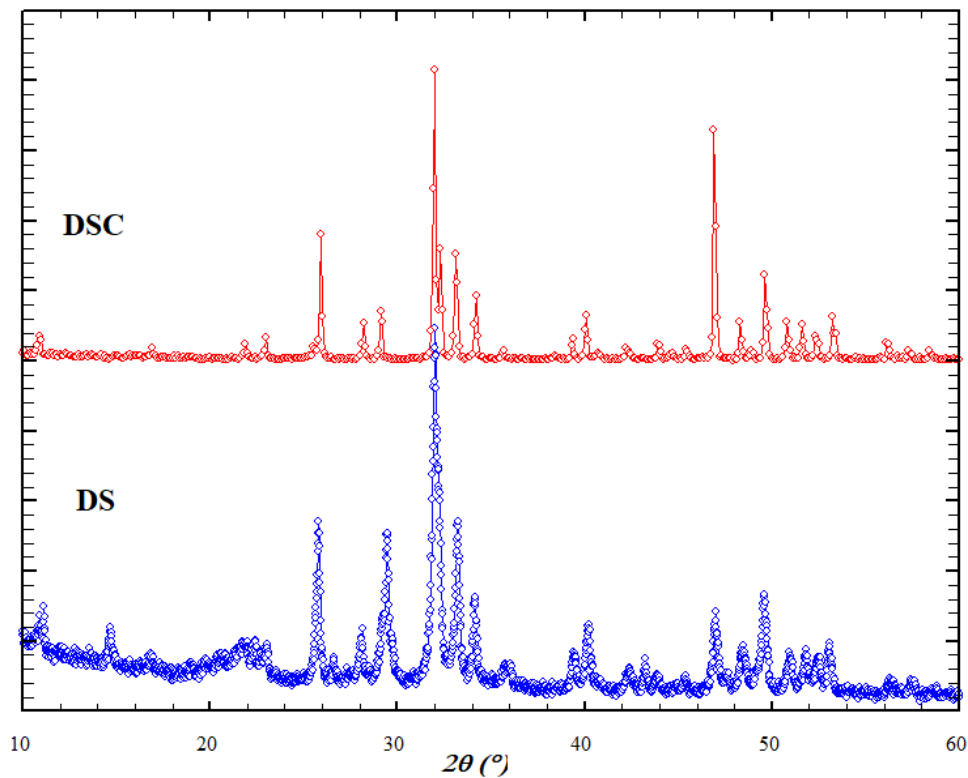


Fig. 3. X-ray diagrams of the adsorbents used.

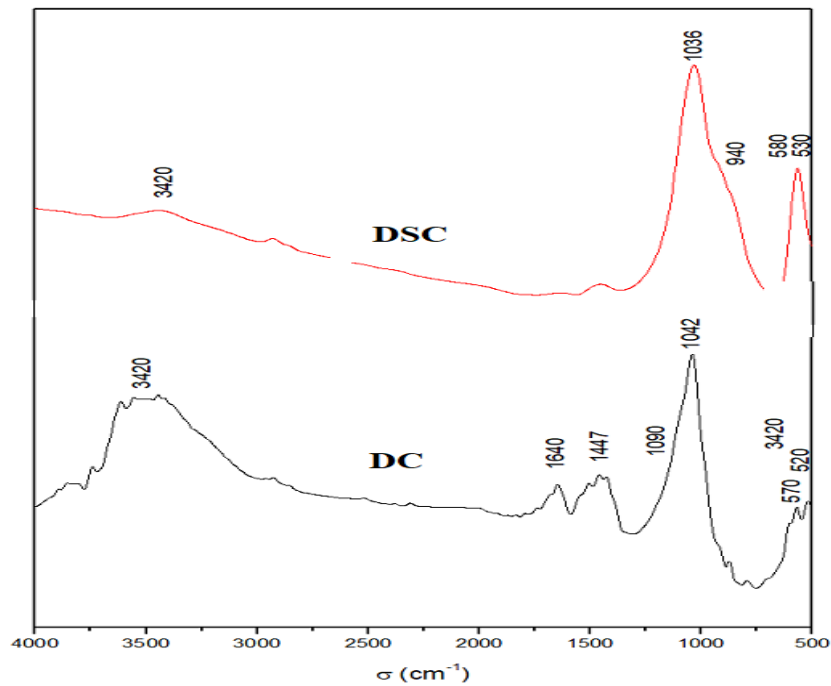


Fig. 4. Infrared absorption spectra of the adsorbents used

The TGA and TDA of the DS samples are shown in Fig. 5. The TGA curve displayed three successive weight losses. The first one occurred between room temperature and 150°C and is related to water volatilization. The second one is due to dehydration from 170 to 450°C [28,42]. The third one, which started at 400°C and ended at 1000°C, was related to the decomposition of carbonates and other materials [42]. The first weight loss is associated with the endothermic effect that is observed on the DTA curve at 85

and 100°C, with a shoulder at 140°C. The second weight-loss coincides with a broad endothermic effect that is evidenced on the DTA curve at around 350°C. Regarding the third weight loss, two broad exothermic peaks were observed in the temperature range of 600-1200°C and are associated with the phase transformation of some resulting products. The DRX and FTIR data confirmed these weight losses.

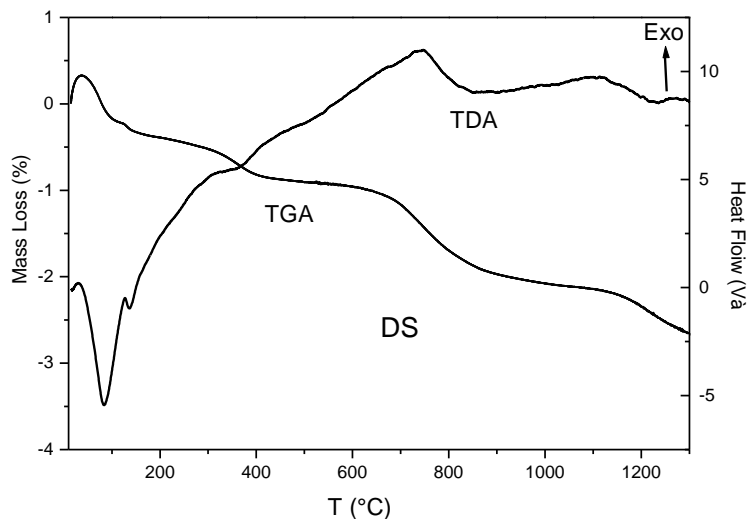


Fig. 5. TGA analysis of the natural phosphate (a, a') and phosphate waste rock (b, b') samples

The TDATG curves of the DSC sample are shown in Fig. 6. For the calcined sample, the presence of a single endothermic peak attributed to the loss of adsorbed water.

In the SEM micrographs, the DC and DSC samples show the presence of nonporous particles of different sizes with spherical shapes. However, in the calcined sample, an improvement of crystallinity, reduced grain size, and an agglomeration of particles was observed (Fig. 7).

The DS and DSC compounds showed specific surface areas of $26.02 \text{ m}^2.\text{g}^{-1}$ and $19.35 \text{ m}^2.\text{g}^{-1}$, respectively. These values are near to those measured for natural phosphate rocks [43]. The

difference between the two SSA values of both materials could be related to the calcination process allowing the easy insertion of N_2 molecules into the adsorbing sites. The average pore volume value increased from 0.052 to 0.041 cc.g^{-1} after calcination, associated with an average pore diameter of 9.58 and 8.02 nm for raw and calcined samples, respectively. This confirms the nonporous character of the used materials. Upon calcination, a decrease of the surface area values was observed when samples were heated at 1000°C . These results are in good agreement with the data described in the literature [44,45]. The decrease of the textural properties indicated that the thermal treatment has modified the adsorption sites to N_2 molecules compared to the original materials.

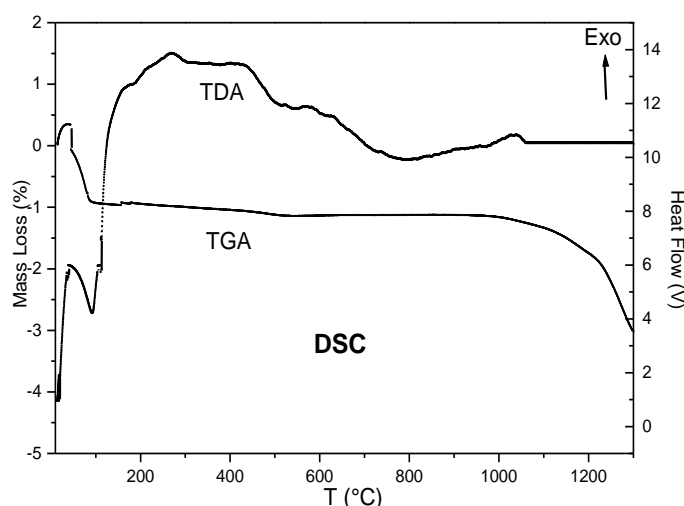


Fig. 6. DTA analysis of the natural phosphate (a, b) and phosphate waste rock (b, b') samples

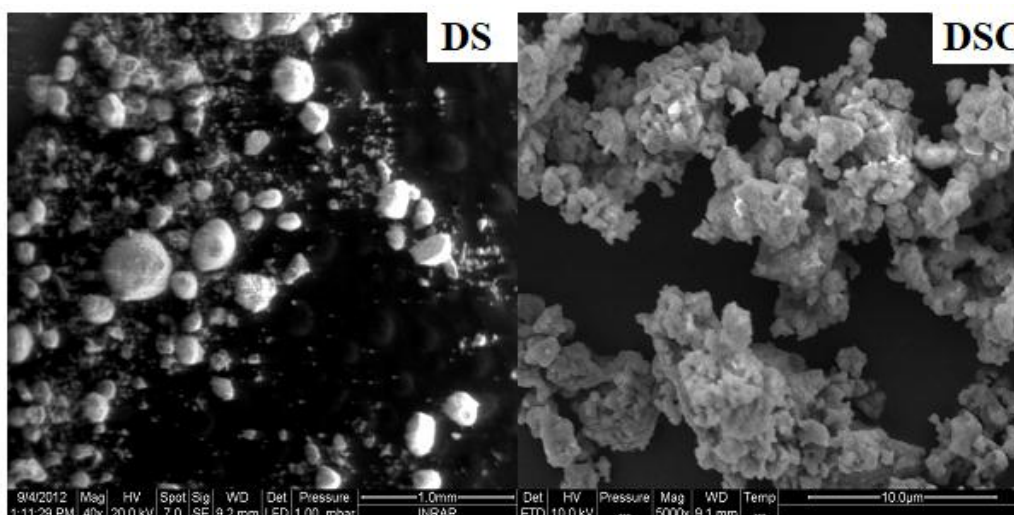


Fig. 7. SEM micrographs of DS and DSC samples

3.2 Effect of Adsorbent Mass

Different amounts of adsorbents were introduced into 200 ml of wastewater discharge with a concentration of Acid Red 52 of 100 mg.L^{-1} . The solution was maintained under stirring at a speed of 100 rpm for 4 hours. Fig. 8 shows that the removal amount of the dye increased with the increase in the adsorbent quantity. Indeed, 0.15 g of DS is sufficient to remove almost 99% of the dye while it takes 0.35 g of DSC to achieve the same result. This behavior is related to the increase in adsorption sites on the surface of the particles following the increase in the amount of adsorbent. The better yield obtained with the DS can be explained by finer particle size and a larger specific surface area of the material and therefore a greater number of adsorption sites. To avoid an adsorbent overdose it is preferable to work with masses less than 0.1 g of DS and 0.35 g of DSC. In fact, larger amounts can lead to agglomeration of the powders and to a reduction in their specific surface.

3.3 pH Effect

Numerous studies have shown that when studying the adsorption of dyes by different adsorbents, the pH of solutions is an important factor to be considered in any adsorption study [36,37].

The suspensions used for the study of the pH influence were prepared by introducing 0.2 g of powder into 200 mL of a solution with a dye concentration of 100 mg.L^{-1} . After adjusting their pH between 3 and 9 using HCl solution (1M), the determination of the supernatant was carried out under the same conditions as above.

Fig. 9, representing the change in the amount of adsorbed acid as a function of pH shows that this amount decreases when the pH of the suspension increases. The dye being acidic, its dissolution in aqueous liberates the anionic ion $\phi\text{-SO}^{3-}$. As the charge of the adsorbent particles depends on the pH, the increase in the latter is accompanied by an increase in the intensity of the repulsive forces between the anionic fragment of the dye and the surface of the adsorbed particles, which is negatively charged, where the decrease in active sites and in the amounts of adsorbed dye.

3.4 Absorption Kinetics

To approximate the mechanism of adsorption of acid red 52 on the materials used, two kinetic models were tested; first-order [38] and pseudo-second-order [39, 40]. These models were chosen for their simplicity and for their application in the field of adsorption of organic compounds on different adsorbents.

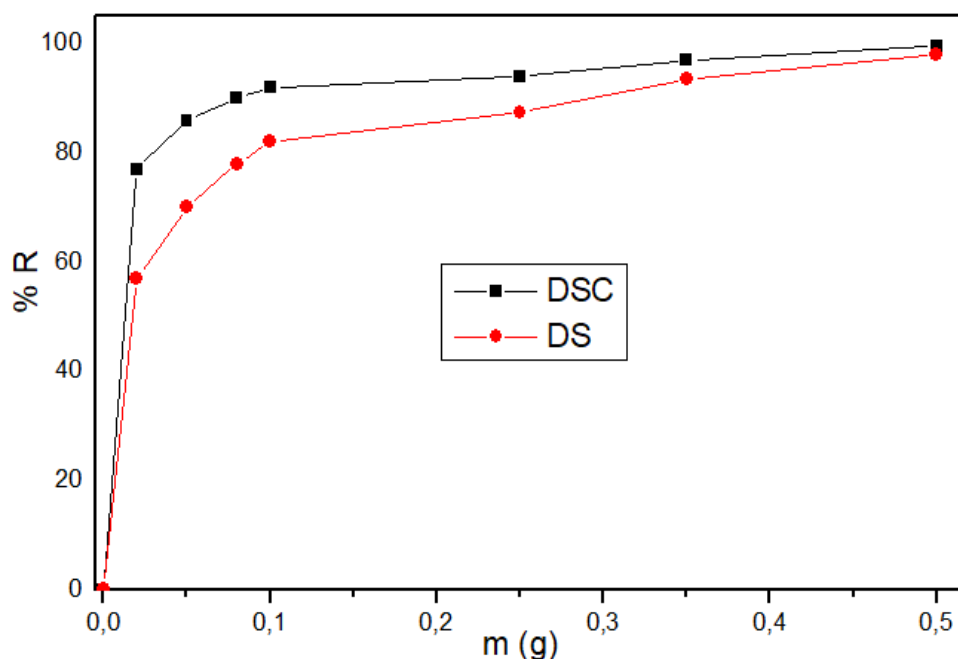


Fig. 8. Percentage of Acid Red 52 retained as a function of the mass of the adsorbent

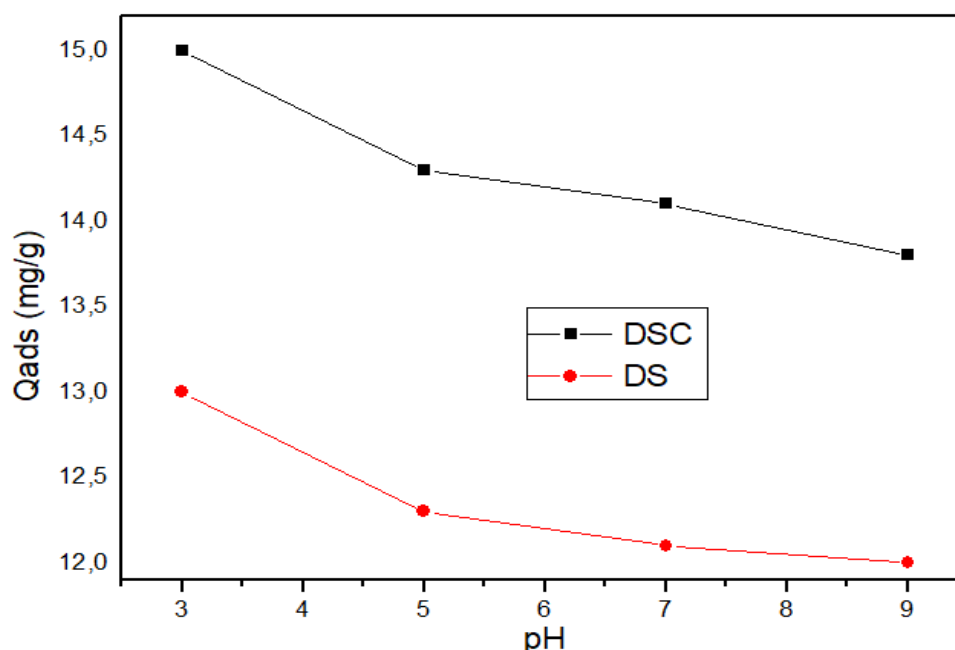


Fig. 9. Evolution of the adsorbed amount of Acid Red 52 as a function of pH

3.4.1 The first-order model

The first-order kinetic model is expressed by the following relation:

$$\frac{dq_t}{dt} = k_1(q_e - q_t) \quad (3)$$

Where q_e and q_t are respectively the quantity of dye (mg.g^{-1}) fixed on the particles of materials at equilibrium and time t and k_1 is the rate constant (min^{-1}). Taking into account the boundary conditions (at $t = 0$, $q_t = 0$ and at $t = t_e$, $q_t = q_e$), the integration of the previous relation gives:

$$\log(q_e - q_t) = \log q_e - \frac{k_1 t}{2,3} \quad (4)$$

The graphical representation of $\log(q_e - q_t)$ as a function of t leads to a line from which the values of k_1 and q_e are determined, respectively using the slope and the y-intercept.

3.4.2 The pseudo second-order model

This model is expressed by the following relation:

$$\frac{dq_t}{dt} = k_2(q_e - q_t)^2 \quad (5)$$

k_2 is the rate constant.

Integration, taking into account the boundary conditions, gives the following equation:

$$\frac{t}{q_t} = \frac{1}{k_2 q_e^2} + \frac{t}{q_e} \quad (6)$$

The rate constant k_2 and the amount of dye fixed at the equilibrium q_e are deduced from the curve $\frac{t}{q_t} = f(t)$, respectively from the slope and the y-intercept.

The dye fixation kinetics, describing the reaction rate, allows the determination of the contact time necessary to reach the adsorption equilibrium. This study was carried out using suspensions prepared by mixing 200 mL of a solution of red acid 52 with a concentration of 100 mg.L^{-1} and 0.2 g of adsorbent, kept under stirring with a speed of 100 rpm. 1 for 400 min.

The results obtained are presented in Fig. 10. It appears that the rate of adsorption is fast at the start of the process and becomes slower over time until equilibrium is achieved. This behavior is to be related to the decrease in active sites on the surface of the particles of materials, following the attachment of increasingly large quantities of

the dye. The times required for the establishment of the absorption equilibrium of the materials are very close and equal to approximately 250 min. It is also noted that the retention capacity of the raw solid waste is greater than that of the calcined solid waste. The quantities used are respectively 14.48 and 11.75 mg.g⁻¹.

The values of the speed constants, deduced from the curves of Figs. 11 and 12 are grouped together with the values of the adsorbed quantities q_e and the regression coefficients R^2 in Tables 2 and 3.

As these tables show, the values of R^2 , obtained by applying the first-order model are relatively low. On the other hand, those deduced from the pseudo-second-order model are greater than 0.99. This indicates that the latter model is the most suitable for determining the order of the absorption kinetics of Red Acid 52 on the used materials. In addition, the values of q_e calculated using this latter model are close to those determined experimentally, confirming the idea that the absorption kinetics of Red 52 acid by the various adsorbents are of pseudo-second order.

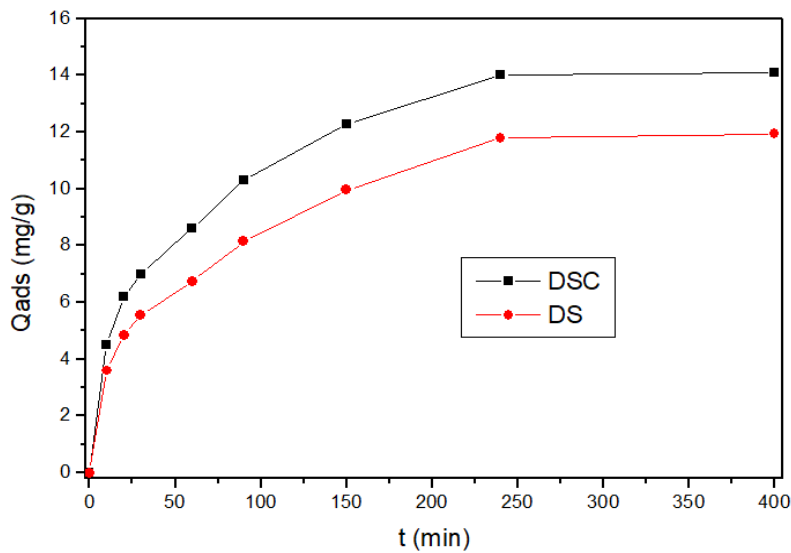


Fig. 10. Evolution of the adsorbed quantity of Acid Red 52 as a function of the contact duration

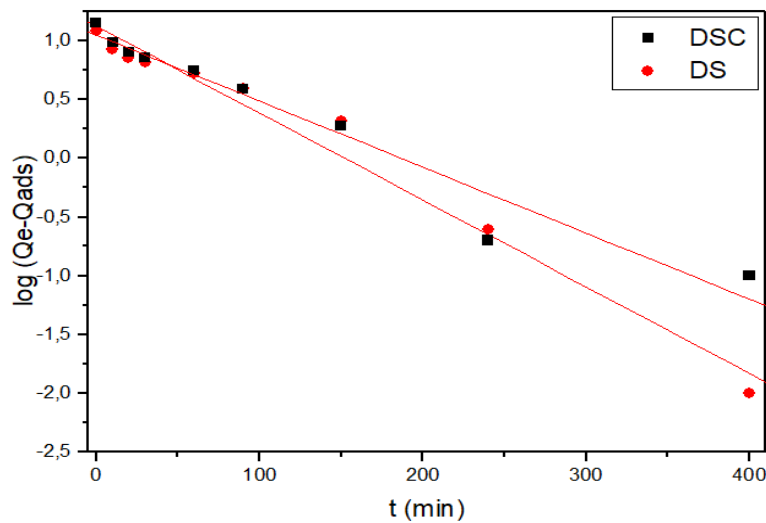


Fig. 11. Linear form plot of the second-order kinetic model by adsorption of the dye on the DS and DSC

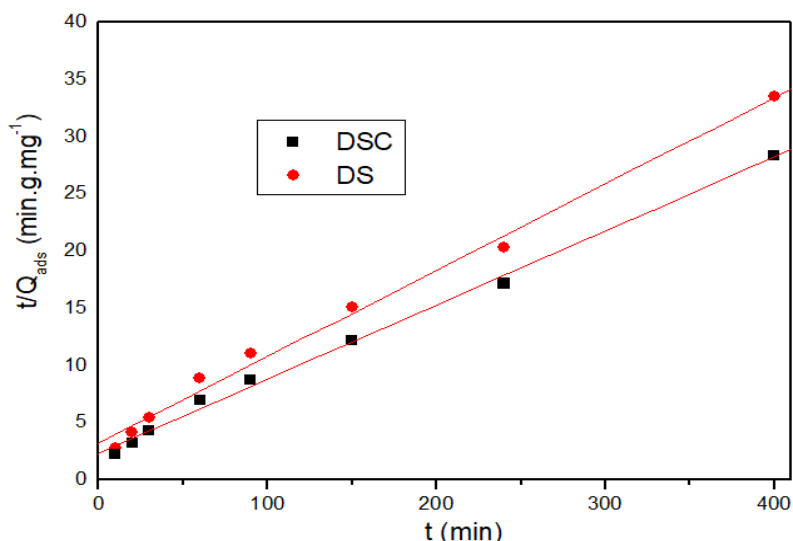


Fig. 12. Linearization of kinetic curves using the pseudo-second-order model

Table 2. Kinetic adsorption parameters according to the first-order model

	K_v (min^{-1})	Q_e théo (mg/g)	Q_{exp} (mg/g)	R^2
DS	0,129	14,20	11,18	0,976
DSP	0,169	12,00	13,24	0,988

Table 3. Kinetic adsorption parameters according to the pseudo second-order model

	K' ($\text{min}^{-1} \text{gmg}^{-1}$)	Q_e théo (mg/g)	Q_{exp} (mg/g)	R^2
DS	$1,69 \cdot 10^{-3}$	14,200	15,41	0,998
DSC	$1,79 \cdot 10^{-3}$	12,00	13,23	0,996

3.5 Adsorption Isotherms

For this study, varying amounts of dye and 0.2 g of adsorbent were dispersed in distilled water. After stirring at a speed of 100 rpm for 4 h, the measurements were carried out according to the protocol indicated above.

The curves shown in Fig. 13, show that the quantity of dye fixed on the adsorbents increases rapidly in low concentrations and decreases as the latter increases. It becomes constant near 150 mg.L^{-1} . For this value, there is a saturation of the adsorption sites and the equilibrium is reached. Efficiency was significantly reduced from 18.4 to 15.2 mg.g^{-1} when the sample was heat-treated at 1000°C .

The variation in the removal properties could be related to the changes on the surfaces of the materials obtained with some loss of the groups necessary for the removal of the acid dye. Indeed, it has been reported that the calcination process generally decreases the capacity to remove other solid wastes [41,42].

The curves' modeling was carried out using the classic models of Langmuir and Freundlich. To develop his model, Langmuir put forward three hypotheses: the adsorption of the adsorbate on the surface of the adsorbent occurs in a single layer, the adsorption takes place at defined sites on the surface of the adsorbent, assumed to be uniform, and the absence of interactions between the adsorbed molecules [43].

According to this model, at a given temperature, the adsorbed quantity q_e is related to the maximum adsorption capacity q_m , to the concentration equilibrium C_e of the adsorbed dye, and to the constant equilibrium characteristic of the adsorbent K_L by the relation:

$$q_e = \frac{q_m K_L C_e}{1 + K_L C_e} \tag{7}$$

Whose linear transform is [44]:

$$\frac{C_e}{q_e} = \frac{C_e}{q_m} + \frac{1}{K_L q_m} \tag{8}$$

The values of q_m and K_L are determined respectively from the intersection with the y-axis

and the slope of the line $\frac{C_e}{q_e} = f(C_e)$.

Unlike Langmuir's, Freundlich's model [45] assumed that the adsorption occurs in multilayers, the surface of the adsorbent is heterogeneous and there are interactions between the adsorbed molecules [46]. It is expressed by the following relation:

$$q_e = K_F C_e^{1/n} \tag{9}$$

Where K_F is the Freundlich constant ($l.g^{-1}$) characterizing the adsorbing power of materials and n is the heterogeneity factor.

The linearization of absorption isotherms according to this model is carried out using the following equation:

$$\ln q_e = \ln K_F + \frac{1}{n} \ln C_e \tag{10}$$

The curves in Fig. 13 show significant adsorption at low concentrations of the dye. The graphical representation of $\ln(q_e)$ as a function of $\ln(C_e)$ is a line whose slope is $1/n$ and the intercept is $\ln(K_F)$.

From Figs. 14 and 15, it appears that for the two materials, the Langmuir model (Fig. 14) leads to a good correlation with the experimental results. The linearization of the absorption isotherms of Red Acid 52 on the two samples is perfect, the correlation coefficients are greater than 0.99 (Table 4).

As expected, the implementation of the Freundlich model leads to low correlation coefficients (Table 5). The values of q_m determined by the Langmuir model are given in Table 4, the Freundlich constants K_f and n_f are grouped together in Table 6.

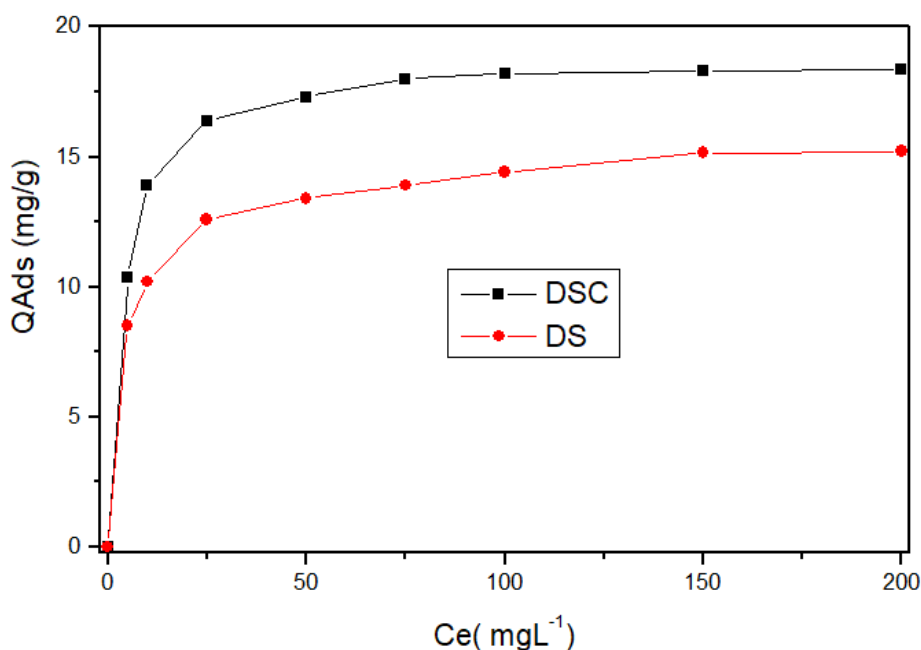


Fig. 13. Adsorption isotherms of Acid Red 52

Table 4. Equilibrium parameters according to the Langmuir model

Adsorbants	q_m (mg/g)	$K_L(L.g^{-1})$	R^2
DS	16.732	0,272	0,999
DSC	14.615	0,155	0,999

Table 5. Equilibrium parameters according to the Freundlich model

Adsorbants	1/n	K_f (L.g ⁻¹)	R ²
DS	0,141	175,822	0,917
DSC	0,154	90,964	0,974

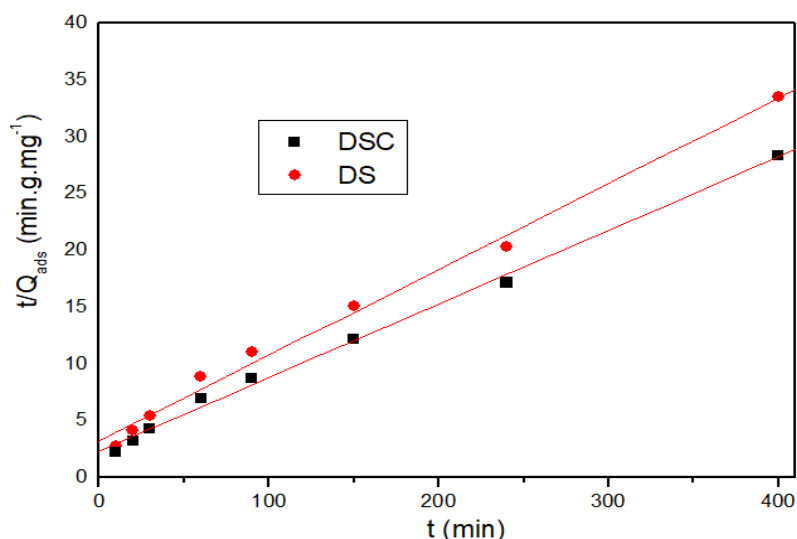


Fig. 14. Modeling of adsorption isotherms according to the Langmuir model

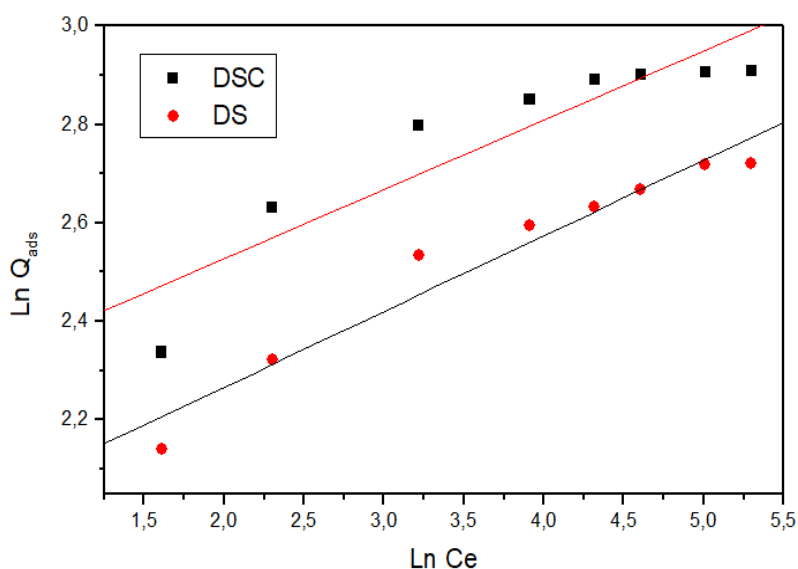


Fig. 15. Modeling of adsorption isotherms according to the Freundlich model

3.6 Temperature Effect

The influence of temperature was studied in the range 35 to 80 °C, using a Mathis type Labomat consisting of 12 bottles. 0.1 g of each of the two adsorbents was dispersed in 100 mL of a solution with a dye concentration of 100 mg.L⁻¹. Before use, the suspensions were kept under stirring at 40 rpm⁻¹ for 1 hour.

Fig. 16 shows the influence of temperature on the adsorption of acid by different materials. It shows that the adsorbed amount decreases with increasing temperature. This decrease suggests that the adsorption process is exothermic.

The thermodynamic quantities ΔG° , ΔH° and ΔS° of the adsorption of the dye on the different

adsorbents were determined using the following equations [47, 48]:

$$\Delta G^{\circ}_{ads} = \Delta H^{\circ}_{ads} + T\Delta S^{\circ}_{ads} \quad (11)$$

$$\Delta G^{\circ}_{ads} = -RT\ln K_c \quad (12)$$

$$\ln K_c = \left(\frac{\Delta S^{\circ}}{R} \right) - \left(\frac{\Delta H^{\circ}}{R} \right) \frac{1}{T} \quad (13)$$

with:

K_c : Distribution coefficient of the dye between the adsorbent and the solution

R : Ideal gas constant ($J \cdot mol^{-1} \cdot K^{-1}$)

T : Absolute temperature (K).

By taking $\ln K_c$ as a function of $1/T$, we obtain a line with the y-intercept $\frac{\Delta S^{\circ}}{R}$ and slope $\frac{-\Delta H^{\circ}}{R}$ (Fig. 17).

The results obtained are grouped in Table 6. The negative values of the three quantities ΔG° , ΔH° and ΔS° indicate that the adsorption of red acid52 on the various adsorbents is spontaneous, exothermic and that the order of distribution of the molecules of the dye on the adsorbent is greater than that in the solution [49, 50]. Furthermore, the ΔH° values obtained for DS and DSC (of the order of $1 \text{ kJ} \cdot \text{mol}^{-1}$) are in favor of physisorption.

The increase in ΔG° values with temperature is related to the increase in disorder during adsorption (Table 7).

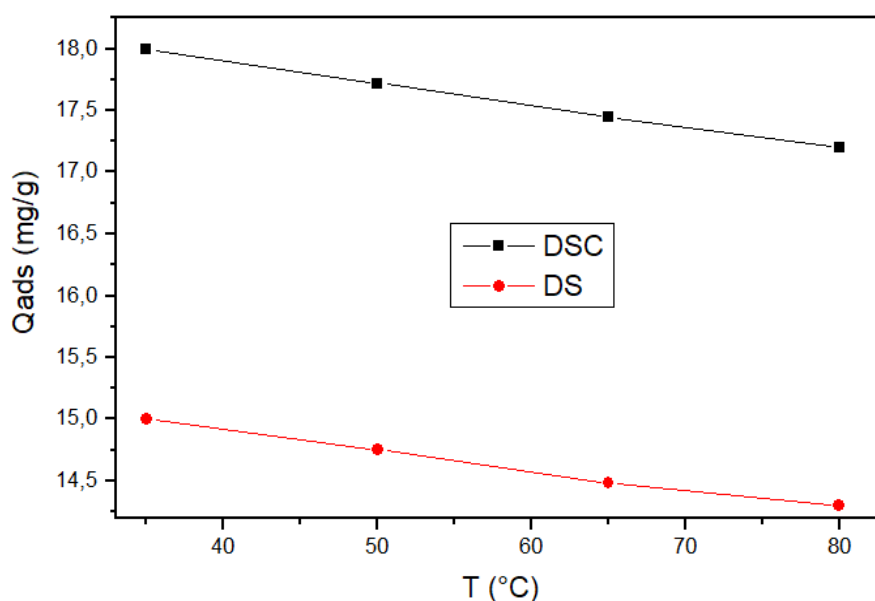


Fig. 16. Influence of temperature on the adsorption of Red Acid 52

Table 6. Thermodynamic adsorption parameters

Adsorbants	ΔH° ($\text{kJ} \cdot \text{mol}^{-1}$)	ΔS° ($\text{J} \cdot \text{K} \cdot \text{mol}^{-1}$)	R^2
DS	-1,10	-16,20	0,999
DSC	-1,13	-18,08	0,998

Table 7. Standard free enthalpy of adsorption

ΔG° ($\text{kJ} \cdot \text{mol}^{-1}$)	T (K)	308	323	338	353
	Adsorbants	DS	-6,09	-6,33	-6,57
	DSC	-6,70	-6,97	-7,24	-7,51

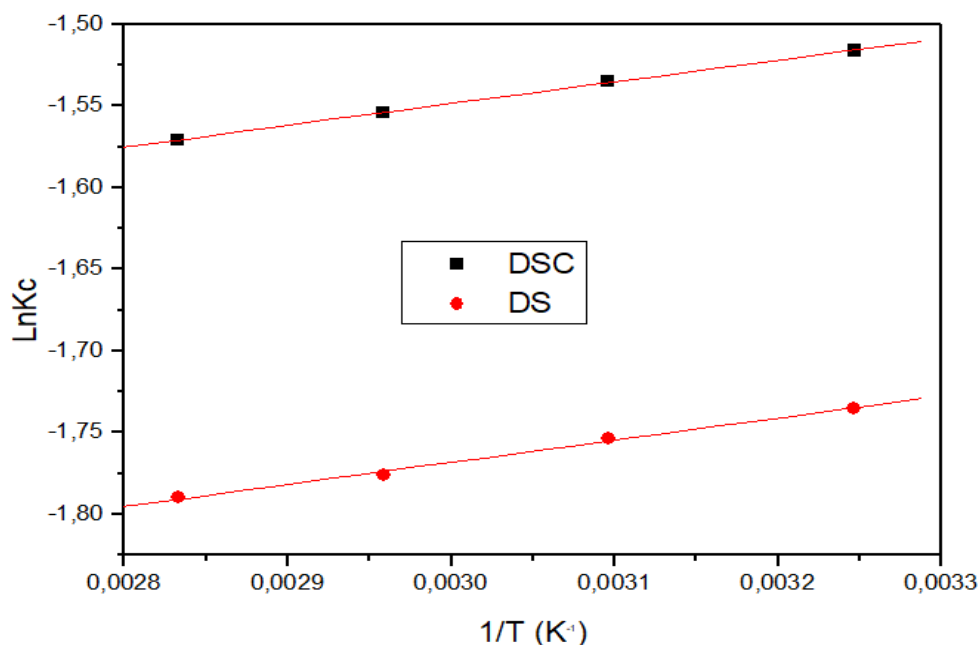


Fig. 17. Determination of the enthalpies and entropies of the Red Acid 52 adsorption

4. CONCLUSION

The solid wastes of the phosphate industry resulting from the washing of rock phosphate, studied in this work, are found in abundance in Tunisia country and are free, their inconvenient of expensive storage. This shows that it is possible to recover these harmful materials in the de-pollution of wastewater from the textile industry, loaded with dyes. Indeed, the tests revealed that Red Acid 52 has been successfully retained on the solid waste of the phosphate industry used. The results obtained also indicated that the solid waste from washing the uncalcined rock phosphate has the best adsorption capacity of 18.4 mg.g^{-1} . The retained quantity decreases when the adsorbent is calcined. The most appropriate model to understand the experimental results of the adsorption kinetics on the two adsorbents is the pseudo-second-order model. As for the adsorption isotherms, they are well described by the Langmuir model. The study of the effect of temperature on the adsorption of 52 acids by solid waste from the washing of calcined and uncalcined rock phosphate, shows a decrease in the amount adsorbed with increasing temperature. Furthermore, the determination of the thermodynamic quantities shows that the adsorption is spontaneous and exothermic. The values of the enthalpy of adsorption indicate that this reaction is physical in nature for both materials.

DISCLAIMER

This paper is an extended version of a preprint document of the same author.

The preprint document is available in this link: <https://www.preprints.org/manuscript/202112.0319/v1>

[As per journal policy, pre-print article can be published as a journal article, provided it is not published in any other journal]

COMPETING INTERESTS

Authors have declared that no competing interests exist. The products used for this research are commonly and predominantly use products in our area of research and country. There is absolutely no conflict of interest between the authors and producers of the products because we do not intend to use these products as an avenue for any litigation but for the advancement of knowledge. Also, the research was not funded by the producing company rather it was funded by personal efforts of the authors.

REFERENCES

1. Rossner A, Snyder SA, Knappe DRU. Knappe, Removal of emerging

- contaminants of concern by alternative adsorbents. *Water Res.* 2009;43:3787.
2. Venkata Mohan S, Sailaja P, Srimurali M, Karthikeyan. Colour removal of monoazo acid dye from aqueous solution by adsorption and chemical coagulation. *J. Environ. Eng. Policy.* 1999; 1:149.
 3. Shin HS, Lee JK. Performance evaluation of electrocoagulation and electrode-watering system for reduction of water content in sewage sludge. *Korean J. Chem. Eng.* 2006;23(2):188.
 4. Crini G. Non-conventional low-cost adsorbents for dye removal. *Bioresource Technol.* 2006;97: 106.
 5. Muthukumar M, Sargunamani D, Selvakumar N. Statistical analysis of the effect of aromatic, azo and sulphonic acid groups on decolouration of acid dye effluents using advanced oxidation processes. *Dyes Pigments.* 2005;65: 151.
 6. Muthukumar M, Sargunamani D, Senthilkumar M, Selvakumar N. Studies on decolouration, toxicity and the possibility for recycling of acid dye effluents using ozone treatment. *Dyes Pigments.* 2005;64: 39.
 7. Khehra MS, Saini HS, Sharma DK, Chadha BS, Chimni SS. Biodegradation of azo dye C.I. Acid Red 88 by an anoxic-aerobic sequential bioreactor, *Dyes Pigments.* 2006;70:1-7.
 8. O'Neill C, Lopez A, Esteves S, Hawkes FR, Hawkes DL, Wilcox S. Azo-dye degradation in an anaerobic-aerobic treatment system operating on simulated textile effluent, *Appl. Microbiol. Biot.* 2000; 53(2):249.
 9. Sharma DK, Saini HS, Singh M, Chimni SS, Chadha BS. Biological treatment of textile dye Acid violet-17 by bacterial consortium in an up-flow immobilized cell bioreactor *Lett. Appl. Microbiol.* 2004;38: 345.
 10. El-Geundi MS. Colour removal from textile effluents by adsorption techniques. *Water Res.* 1991;25 271.
 11. Nassar MM, Hamoda MF, Radwan GH. Adsorption equilibria of basic dyestuff onto palm-fruit bunch particles. *Water Sci. Technol.* 1995;32:27.
 12. Nassar MM, Magdy YH. Removal of different basic dyes from aqueous solutions by adsorption on palm-fruit bunch particles. *Chem. Eng. J.* 1997; 66:223.
 13. Nassar MM. Intraparticle diffusion of basic red and basic yellow dyes on palm fruit bunch. *Water Sci. Technol.* 1999;40:133.
 14. Morais LC, Freitas OM, Gon Calves EP, Vasconcelos LT, Gonzalez CG. Reactive dyes removal from wastewaters by adsorption on eucalyptus bark: variables that define the process *Water Res.* 1999;33: 979.
 15. Padmesh TVN, Vijayaraghavan K, Sekaran G, Velan M. Application of Azolla rongpong on biosorption of acid red 88, acid green 3, acid orange 7 and acid blue 15 from synthetic solutions. *Chem. Eng. J.* 2006; 22: 55.
 16. Gupta VK, Mohan D, Sharma S, Sharma M. Removal of Basic Dyes (Rhodamine-B and Methylene Blue) from Aqueous Solutions Using Bagasse Fly Ash. *Separ. Sci. Technol.* 2000;35:2097.
 17. Liversidge RM, Lloyd GJ, Wase DAJC, Forster F. Removal of Basic Blue 41 dye from aqueous solution by linseed cake. *Process Biochem.* 1997;32:473.
 18. Ann Adurai G, Juang RS, Lee DJ Use of cellulose-based wastes for adsorption of dyes from aqueous solutions *J. Hazard. Mater.* 2002;B 92:263.
 19. Raïs Z, El Hassani L, Maghnouje J, Hadji M, Ibnelkhayat R, Nejjar R, Kherbeche A, Chaqroune A. Dyes' removal from textile wastewater by phosphogypsum using coagulation and precipitation method. *Phys. Chem. News.* 2002;7:100.
 20. Barka N, Assabbane A, Nounah A, Laanab L, Aït Ichou Y. Removal of textile dyes from aqueous solutions by natural

- phosphate as a new adsorbent Desalination. 2009;235:264.
21. Achkoun A, Naja J, Hamdi RM. Elimination of cationic and anionic dyes by natural phosphate. *J. Chem. Chem. Eng.* 2012;6:721.
 22. Jha P, Jobby RN, Desai S. Remediation of textile azo dye acid red 114 by hairy roots of *Ipomoea carnea* Jacq. and assessment of degraded dye toxicity with human keratinocyte cell line. *J. Hazard. Mater.* 2016;311: 158.
 23. Hussain G, Ather M, Ul Ain Khan M, Saeed A, Saleem R, Shabir G, Ali Channar P. *Dyes Pigments.* 2005; 65: 151.
 24. Mizane A, Louhi A. Calcination effects on sulfuric dissolution of phosphate extracted from djebel onk mine (Algeria), *Asian J. Chem.* 2008;20:711-717.
 25. Elliott JC. *Structure and chemistry of the apatites and other calcium orthophosphates*, Elsevier, Amsterdam; 1994.
 26. Raynaud S, Champion E, Bernache-Assollant D, Thomas P. *Biomaterials.* 2002; 23: 1065.
El Hammari L, Merroun H, Coradin T, Laghizil A, Barboux P, Saoiabi A. Mesoporous hydroxyapatites prepared in ethanol-water media: Structure and surface properties. *Mater. Chem. Phys.* 2007; 104:448.
 27. Feki EH, Savariault JM, Ben Salah A. Structure refinements by the Rietveld method of partially substituted hydroxyapatite: $\text{Ca}_9\text{Na}_{0.5}(\text{PO}_4)_{4.5}(\text{CO}_3)_{1.5}(\text{OH})_2$ *J. Alloys Compd* 1999;287:114.
 28. Lafon JP, Champion E, Bernache-Assollant D. Processing of AB-type carbonated hydroxyapatite $\text{Ca}_{10-x}(\text{PO}_4)_{6-x}(\text{CO}_3)_x(\text{OH})_{2-x-2v}(\text{CO}_3)_v$ ceramics with controlled composition. *J. Eur. Ceram. Soc.* 2008;28:139.
 29. Gmati N, Boughzala K, Abdellaoui M, Bouzouita K, Chimie CR. Mechanochemical synthesis of strontium britholites: Reaction mechanism. 2011;14:896.
 30. Elliott JC. *The crystallographic structure of dental enamel and related apatites.* PhD Thesis, University of London; 1994.
 31. Elliott JC. *The crystallographic structure of dental enamel and related apatites.* PhD Thesis, University of London; 1994.
 32. El Boujaady H, El Rhilassi A, Bennani-Ziatni M, El Hamri R, Taitai A, Lacout JL. Removal of a textile dye by adsorption on synthetic calcium phosphates, *Desalination.* 2011;275:10-16.
 33. Kooli F, Yan L, Al-Faze R, Al Suhaimi A. Effect of acid activation of Saudi local clay mineral on removal properties of basic blue 41 from an aqueous solution, *Applied Clay Sci.* 2015;116-117:23-30.
 34. Lagergren S, Vetenskapsakad S. *Zur Theorie der Sogenannten Adsorption Gelöster Stoffe*, Kungliga Svenska Vetenskapsakademiens. Hand. Band. 1898;24(4):1.
 35. Ho YS, Mc Kay G. The kinetics of sorption of divalent metal ions onto sphagnum moss peat *Water Res.* 2000;34(3):735.
Ho YS, Mc Kay G. Pseudo-second order model for sorption processes. *Process Biochem.* 1999 ; 34:451.
 36. Vimonses V, Jin B, Chow CWK, Saint C. Enhancing removal efficiency of anionic dye by combination and calcination of clay materials and calcium hydroxide, *J. Hazard. Mater.* 2009; 171: 941-947.
 37. Graba Z, Hamoudi S, Bekka D, Bezzi N, Boukherroub R. Influence of adsorption parameters of basic red dye 46 by the rough and treated Algerian natural phosphates, *J. Ind Eng. Chem.* 2015;25: 229-238.
 38. Langmuir L. The adsorption of gases on plane surfaces of glass, mica and platinum. *J. Am. Chem. Soc.* 1918;40: 1361.
 39. Stumm W, Morgan JJ. *An introduction emphasizing chemical equilibria in natural waters.* Aquatic chemistry, Ed.2, Wiley inter-science J., Wiley & Sons; 1981.
 40. Freundlich H. *Colloid and Capillary Chemistry.* Methuen, London; 1926.
 41. Mc Kay G. *Use of adsorbents for the removal of pollutants from wastewaters.* CRC Press; 1996.
 42. Abd El-Rahman KM, El-Kamash AM, El-Sourougy MR, Abdel-Moniem NM. Thermodynamic modeling for the removal of Cs^+ , Sr^{2+} , Ca^{2+} and Mg^{2+} ions from aqueous waste solutions using zeolite A *J. Radioanal. Nucl. Ch.* 2006; 268: 221.
 43. Demirbas A, Sari A, Isildak O, Adsorption thermodynamics of stearic acid onto bentonite *Hazard J. Mater.* 2006;135, 226.

- Rytwo G, Ruiz-Hitzky E. Enthalpies of adsorption of methylene blue and crystal violet to montmorillonite. *J. Therm. Anal. Calorim.* 2003;71: 751.
44. Ramesh A, Lee DJ, Wong JW. Thermodynamic parameters for adsorption equilibrium of heavy metals and dyes from wastewater with low cost adsorbents. *J. Colloid. Interf. Sci.* 2005;291:588.

© 2021 Mehnaoui et al.; This is an Open Access article distributed under the terms of the Creative Commons Attribution License (<http://creativecommons.org/licenses/by/4.0>), which permits unrestricted use, distribution, and reproduction in any medium, provided the original work is properly cited.

Peer-review history:

The peer review history for this paper can be accessed here:
<https://www.sdiarticle5.com/review-history/85174>